



HypoxamiRs Profiling Identify miR-765 as a Regulator of the Early Stages of Vasculogenic Mimicry in SKOV3 Ovarian Cancer Cells

Yarely M. Salinas-Vera¹, Dolores Gallardo-Rincón², Raúl García-Vázquez³, Olga N. Hernández-de la Cruz¹, Laurence A. Marchat³, Juan Antonio González-Barrios⁴, Erika Ruíz-García², Carlos Vázquez-Calzada⁵, Estefanía Contreras-Sanzón¹, Martha Resendiz-Hernández¹, Horacio Astudillo-de la Vega⁶, José L. Cruz-Colín⁷, Alma D. Campos-Parra⁸ and César López-Camarillo^{1*}

OPEN ACCESS

Edited by:

Monica Venere,
The Ohio State University,
United States

Reviewed by:

Gareth I. Owen,
Pontificia Universidad Católica de
Chile, Chile
Vijay Pandey,
National University of Singapore,
Singapore

*Correspondence:

César López-Camarillo
genomicas@yahoo.com.mx

Specialty section:

This article was submitted to
Cancer Molecular Targets and
Therapeutics,
a section of the journal
Frontiers in Oncology

Received: 09 January 2019

Accepted: 23 April 2019

Published: 14 May 2019

Citation:

Salinas-Vera YM, Gallardo-Rincón D, García-Vázquez R, Hernández-de la Cruz ON, Marchat LA, González-Barrios JA, Ruíz-García E, Vázquez-Calzada C, Contreras-Sanzón E, Resendiz-Hernández M, Astudillo-de la Vega H, Cruz-Colín JL, Campos-Parra AD and López-Camarillo C (2019) HypoxamiRs Profiling Identify miR-765 as a Regulator of the Early Stages of Vasculogenic Mimicry in SKOV3 Ovarian Cancer Cells. *Front. Oncol.* 9:381. doi: 10.3389/fonc.2019.00381

¹ Posgrado en Ciencias Genómicas, Universidad Autónoma de la Ciudad de México, Mexico City, Mexico, ² Laboratorio de Medicina Translacional y Departamento de Tumores Gastro-Intestinales, Instituto Nacional de Cancerología, Mexico City, Mexico, ³ Programa en Biomedicina Molecular y Red de Biotecnología, Instituto Politécnico Nacional, Mexico City, Mexico, ⁴ Laboratorio de Medicina Genómica, Hospital Regional 1 de Octubre ISSSTE, Mexico City, Mexico, ⁵ Departamento de Infectómica y Patogénesis Molecular, CINVESTAV-IPN, Mexico City, Mexico, ⁶ Laboratorio de Investigación Translacional en Cáncer y Terapia Celular, Hospital de Oncología, Centro Médico Nacional Siglo XXI, Mexico City, Mexico, ⁷ Subdirección de Investigación Básica, Instituto Nacional de Medicina Genómica, Mexico City, Mexico, ⁸ Laboratorio de Genómica, Instituto Nacional de Cancerología, Mexico City, Mexico

Vasculogenic mimicry (VM) is a novel cancer hallmark in which malignant cells develop matrix-associated 3D tubular networks with a lumen under hypoxia to supply nutrients needed for tumor growth. Recent studies showed that microRNAs (miRNAs) may have a role in VM regulation. In this study, we examined the relevance of hypoxia-regulated miRNAs (hypoxamiRs) in the early stages of VM formation. Data showed that after 48 h hypoxia and 12 h incubation on matrigel SKOV3 ovarian cancer cells undergo the formation of matrix-associated intercellular connections referred hereafter as 3D channels-like structures, which arose previous to the apparition of canonical tubular structures representative of VM. Comprehensive profiling of 754 mature miRNAs at the onset of hypoxia-induced 3D channels-like structures showed that 11 hypoxamiRs were modulated (FC > 1.5; $p < 0.05$) in SKOV3 cells (9 downregulated and 2 upregulated). Bioinformatic analysis of the set of regulated miRNAs showed that they might impact cellular pathways related with tumorigenesis. Moreover, overall survival analysis in a cohort of ovarian cancer patients ($n = 485$) indicated that low miR-765, miR-193b, miR-148a and high miR-138 levels were associated with worst patients outcome. In particular, miR-765 was severely downregulated after hypoxia (FC < 32.02; $p < 0.05$), and predicted to target a number of protein-encoding genes involved in angiogenesis and VM. Functional assays showed that ectopic restoration of miR-765 in SKOV3 cells resulted in a significant inhibition of hypoxia-induced 3D channels-like formation that was associated with a reduced number of branch points and patterned tubular-like structures. Mechanistic studies confirmed that miR-765 decreased the levels of VEGFA, AKT1 and SRC- α transducers and exerted a negative regulation of VEGFA by specific binding to its 3'UTR. Finally, overall survival analysis of a cohort of ovarian cancer

patients ($n = 1435$) indicates that high levels of VEGFA, AKT1 and SRC- α and low miR-765 expression were associated with worst patients outcome. In conclusion, here we reported a novel hypoxamiRs signature which constitutes a molecular guide for further clinical and functional studies on the early stages of VM. Our data also suggested that miR-765 coordinates the formation of 3D channels-like structures through modulation of VEGFA/AKT1/SRC- α axis in SKOV3 ovarian cancer cells.

Keywords: ovarian cancer, vasculogenic mimicry, hypoxia, miR-765, VEGFA

INTRODUCTION

Tumor vasculogenic mimicry (VM) is a novel cancer hallmark formerly described in malignant melanoma cells which involves the formation of patterned three dimensional (3D) channels networks by tumor cells (1). These tubular networks resemble embryonic vasculogenesis, and they describe the ability of certain types of aggressive cancer cells to express endothelium-associated genes (2). Tumor VM occur *de novo* without or in combination with blood vessels formation changing our conventional acceptance that classical angiogenesis is the only means by which cancer cells acquire a nutrients supply to nourish tumors. Studies supporting these assumptions have demonstrated that *in vivo* the 3D channels contain plasm, erythrocytes and blood flow with a hemodynamics similar to those occurring in endothelial vessels (3). Evidences for VM have been found in other solid tumors and cancer cell lines such as in glioblastoma (4), breast (5, 6), prostate (7), lung (8), hepatocellular (9) and ovarian cancers (10, 11), among others. This morphologic plasticity have been associated to aggressive tumor phenotypes, increased metastasis and tumor progression of certain types of cancers. Moreover, meta-analysis studies have established a definitive association between VM with poor clinical poor prognosis in human cancer patients (12). Remarkably, tumor VM may contribute to the resistance of diverse type of tumors against anti-angiogenic therapy (13, 14). Therefore, the exploration of the multiple roles of VM in cancer hallmarks, especially in drug resistance, would broaden our knowledge and eventually ameliorate the treatment efficacy in cancer.

Cellular features underlying VM are diverse although they may summarized as follows: (i) vascular-like tubules are lined by tumor cells in combination or not with endothelial cells forming complex 3D mosaic patterns; (ii) VM cells achieve remodeling of extracellular matrix and tumor microenvironment; (iii) 3D channels assembled during VM connects with the tumor microcirculation system providing blood and supplies for tumor growth, (iv) VM provides also a perfusion route for metabolic waste; and (v) in tumor tissues VM cells showed Periodic-acid Schiff (PAS) positive and CD31 negative staining which provides a new tool for potential use in clinical practice (15). Nonetheless, *in vitro* reports on VM are still debatable because only few studies provide solid evidence of 3D tube formation (1, 16–19) or use malignant melanoma or ovarian cancer cell lines previously confirmed to form tubular 3D structures (19–21). In an outstanding paper from Owen's lab

this controversy was addressed by characterizing VM *in vitro* using SKOV3, HEY and other ovarian cancer cell lines, as well as spheres and primary cultures derived from ovarian cancer ascites (19). Using dye microinjection, X-ray microtomography 3D-reconstruction, and confocal microscopy studies they confirmed that glycoprotein-rich lined 3D tubular structures are present in *in vitro* cultures and were able of conducting fluids. This study highlights the importance of confirmatory *in vitro* assays for VM, and surprisingly suggested that many of 3D cellular networks reported in the literature may not represent genuine VM (19).

Diverse molecular mechanisms and signaling pathways have been described to be involved in VM formation (22–24). Moreover, it has been described that aggressive tumor cells undergoing VM showed specific gene-expression profiles that resembles that of an undifferentiated, embryonic-like cells (2). Molecular mechanisms operating in VM have been extensively studied recently with some master regulators identified (25). For instance, hypoxia inducible factor 1- α (HIF-1 α) greatly promotes VM formation in response to hypoxia as it occurs in angiogenesis (26). The role of other proteins and signaling pathways that promote cell proliferation, migration, invasion and matrix remodeling during tumor VM also has been described. These include factors such as the vascular endothelial-cadherin (VE-cadherin) (21, 27), epithelial cell kinase (EphA2) (18), phosphoinositide 3-kinase alpha (PI3K- α) (6), matrix metalloproteinase (MMPs), laminin 5 (Ln-5) γ 2 chain, focal adhesion kinase (FAK) (23–25) and proto-oncogene tyrosine-protein kinase SRC- α (6). Although important advances in deciphering the molecular mechanism underlying VM, the fine-tuning modulation and the role of non-coding RNAs in the early stages of VM remains poorly understood.

During the last decades, the study of non-coding RNAs in cancer biology has exploded revealing unsuspected functions in tumorigenesis. MicroRNAs (miRNAs) are non-coding single-stranded small RNAs of 21–25 nucleotides in length that function as negative regulators of gene expression (28). MiRNAs function as guide molecules in post-transcriptional gene silencing by partially complementing with the 3'-end of target transcripts resulting in mRNA degradation or translational repression in cytoplasmic P-bodies (29). These small non-coding RNAs may target a plethora of regulatory molecules driving tumorigenesis. Recent studies showed that some miRNAs have a pivotal role in VM in diverse types of solid tumors. For instance, miR-26b targets EphA2 a VM regulator in glioma (30). In breast cancer, miR-204 exerts a fine-tuning regulation of the synergistic transduction of PI3K/AKT1/FAK mediators critical in VM

formation (6). In ovarian cancer only two studies about the role of miRNAs, specifically miR-200a and miR-27b, have been reported (31, 32), indicating that detailed miRNAs functions in VM regulation in ovarian cancer remains to be elucidated. In the present investigation, we reported a novel miRNAs signature activated during the hypoxia-induced 3D channels-like networks formation in ovarian cancer cells. Also, we provide functional data suggesting a role for miR-765 in VM through regulation of VEGFA/AKT1/SRC- α axis.

MATERIALS AND METHODS

Cell Lines

Human ovarian cancer cell line SKOV-3 was obtained from the American Type Culture Collection (ATTC HTB-77), and routinely grown in Dulbecco's modification of Eagle's minimal medium (DMEM) supplemented with 10% fetal bovine serum and penicillin-streptomycin (50 unit/ml; Invitrogen, Carlsbad, CA, USA).

Periodic Acid Staining

3D-cultures were fixed in 4% formaldehyde in phosphate buffered solution (PBS) 1X for 30 min at room temperature. Coverslips were incubated with 0.5% periodic acid for 5 min, washed with PBS 1X for 5 min and Schiff reagent for additional 15 min. Then, cells were washed with PBS 1X for 5 min. Later they were incubated with hematoxylin for 1 min and washed in tap water for 5 min. Samples were dehydrated and mounted in coverslip using a synthetic mounting medium for microscopy.

Three Dimensional (3D) Cultures

Experiments were performed with 70–80% confluent cell cultures. 3D cultures were prepared for confocal microscopy analysis as follow: 18 × 18 mm glass coverslips were acetone-washed, air-dried and placed in 6-well culture plates, coated with 50 μ L of Matrigel per coverslip and air-dried for 60 min at room temperature. Cell cultures were trypsinized, and 60,000 cells were resuspended in 200 μ L of culture medium, which was seeded on matrigel-coated coverslips. Cells were incubated at 37°C for 3 h to allow its adhesion to the matrix and then covered with 3 ml of culture medium.

Immunofluorescence Analysis

Briefly, 3D-cultures were fixed in 4% formaldehyde in PBS 1X for 30 min at room temperature. Coverslips were incubated with 0.1% Triton X-100 for 3 min. Following washing with PBS 1X, cells were blocked for 40 min at room temperature with 0.2% BSA in PBS 1X, and incubated with Phalloidin 1X (Abcam, ab235138) for 30 min at room temperature. Stained cells were then washed with PBS 1X for 15 min and mounted for confocal microscopy.

RNA Isolation

Total RNA was extracted using 500 μ l Trizol (Invitrogen, Carlsbad, CA) for 1 × 10⁴ cells/well as described the manufacturer. RNA integrity was assessed using capillary electrophoresis system Agilent 2100 Bioanalyzer. Samples with a RNA integrity >5 were processed.

MicroRNAs Expression Profiling

The Megaplex TaqMan Low-Density Array (TLDA) v 3.0 (Applied Biosystems, Foster City, CA) platform was used to measure the expression of 754 human specific miRNAs in parallel. Briefly, total RNA (600 ng) was retro-transcribed using stem-loop primers specific for each miRNA in order to obtain complementary DNA (cDNA) templates. Subsequently, a pre-amplification step of 12 cycles was included to increase the concentration of low-level miRNAs. The pre-amplified products were loaded into the TLDA and reactions were started using the 7900 FAST real-time thermal cycler (ABI). RNU44 and RNU48 expression was used as internal control. For statistical analysis miRNAs levels were measured by quantitative reverse transcription polymerase chain reaction (qRT-PCR) in TLDA using the comparative Ct (2 $\Delta\Delta$ Ct) method. All analyses were done using R (HTqPCR and gplots-bioconductor). The Ct raw data were determined using an automatic baseline and a threshold of 0.2. A fold change (FC) (log₂ RQ) value >1.5 was used to define the differentially expressed miRNAs. An adjusted *t*-test was used to evaluate the significant differences in Ct values between groups. To identify subgroups defined by miRNA expression profiles, an unsupervised clustering analysis using Spearman correlation and average linkage was used.

Bioinformatics Analysis

MiRNA targets were identified using TargetScan 7.0 (http://www.targetscan.org/vert_71/), and PicTar (<http://www.pictar.org/>) softwares. Only target genes that were predicted by the two algorithms were selected for further analysis. Gene ontology and enrichment cellular pathway analyses were performed using David tool.

Transfection of miR-765 Mimic

MiRNA-765 mimic (AM17100 ThermoFisher), and pre-miR-negative control scramble (AM17110 ThermoFisher) were transfected in SKOV3 cells using siPORT amine transfection agent. Briefly, miR-765 (80 nM) and scramble (80 nM) were individually added to wells containing 1 × 10⁴ cells cultured in DMEM for 48 h. Then, overexpression of miR-765 was confirmed by quantitative RT-PCR at 48 h posttransfection using total RNA. MiR-765-expressing cells were used for downstream analysis.

3D Channels-Like Networks Inhibition Assays

3D channels-like networks experiments were performed through 3D-dimensional cultures on matrigel. Firstly, SKOV3 cells (1 × 10⁴ cells/well) were transfected with pre-miR-765 (80 nM) or scramble (30 nM) negative control as previously described. The cells were cultured in 96-well plate covered with geltrex matrix (50 μ l). Afterward, cells were incubated at 37°C in 5% CO₂ atmosphere in hypoxia conditions (1% O₂) for 48 h. Then, the formation of 3D channels formation was induced by seeding cells on matrigel and then capillary-like structures were observed under an inverted microscope (Iroscope SI-PH) and imaged during 0, 6, and 12 h. Two observers individually counted the number of branch points and tubular structures.

Data were expressed as mean \pm S.D. $p < 0.05$ was considered as statistically significant.

Western Blot Assays

30 μ g of whole protein extracts were separated on 12% SDS-PAGE and transferred to 0.2 μ m nitrocellulose membrane (Bio-Rad) and then incubated with the following primary antibodies: anti-AKT1 (1:1000, C74H10 Cell signaling), anti-SRC- α (1:1000; sc-130124 Santa Cruz), anti-VEGFA (1:500, ab183100 abcam) and anti-GAPDH (1:1000, sc-365062 Santa Cruz). Densitometry analysis of immunodetected bands in Western blots assays were performed using the public domain myImage Analysis software.

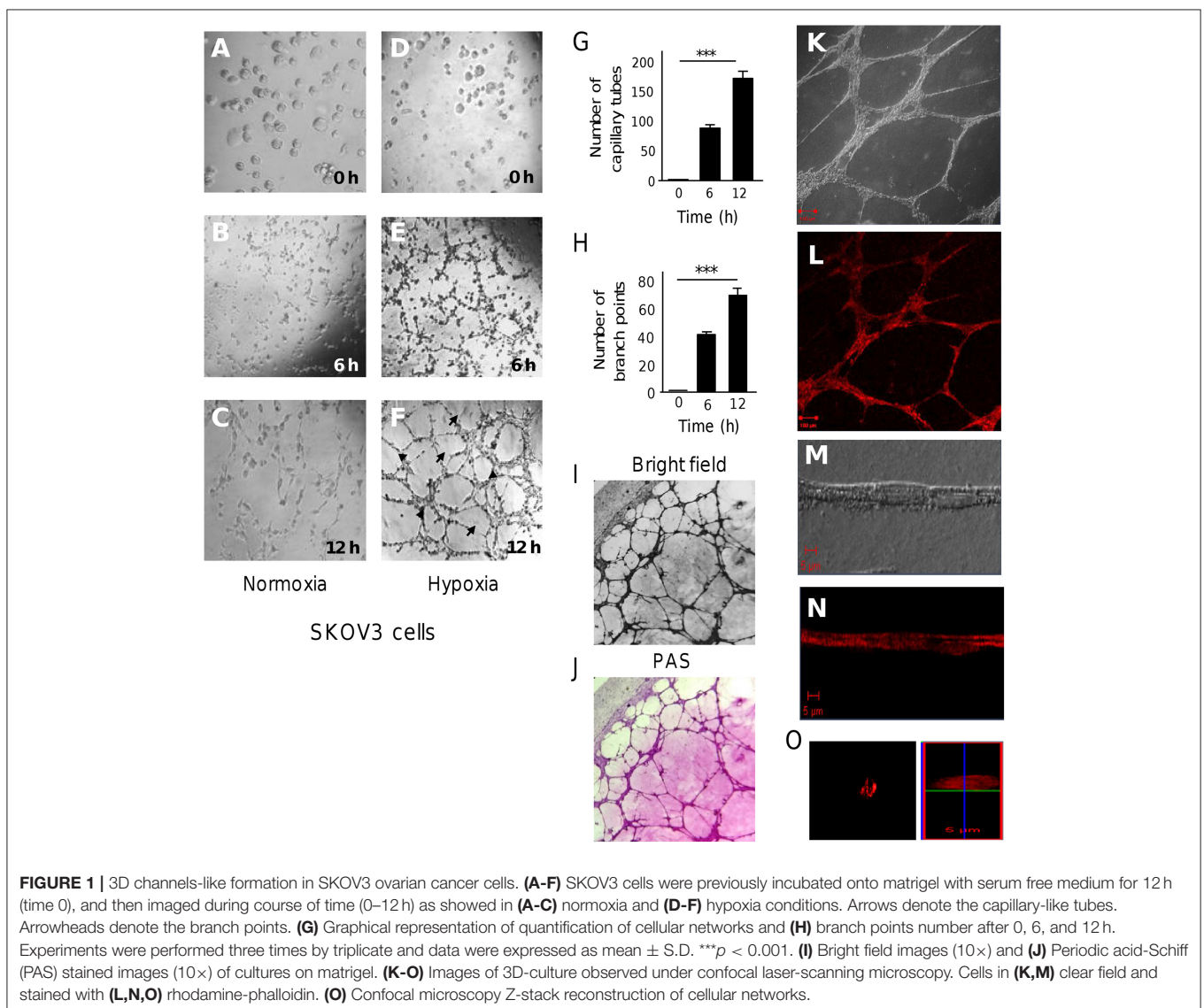
Luciferase Gene Reporter Assays

DNA fragments of the 3'UTR of VEGFA gene containing the predicted miR-765 binding sites were cloned into p-miR-report vector (Ambion) downstream of luciferase gene. All constructs were verified through automatic sequencing. Then, recombinant pmiR-LUC-VEGFA plasmid was transfected into

SKOV3 cells using lipofectamine 2000 (Invitrogen). At 24 h after transfection, pre-miR-765 (80 nM) and scramble were co-transfected with lipofectamine RNAi max (Invitrogen). Then, 24 h after transfection firefly and *Renilla reniformis* luciferase activities were both measured by the Dual-Glo luciferase Assay (Promega) using a Fluoroskan Ascent™ Microplate Fluorometer. Firefly luciferase activity was normalized with *Renilla reniformis* luciferase.

Kaplan Meier Analysis

Overall survival analysis using Kaplan Meier plotter for miR-765, VEGFA, AKT1, and SRC- α genes in ovarian cancer patients were evaluated as previously described (33, 34). Briefly, we used the Start KM plotter for ovarian cancer tool that use genome-wide for mRNA expression data and overall survival clinical information of cancer patients, which were downloaded from Gene Expression Omnibus GEO (Affymetrix HG-U133A, HG-U133A 2.0, and HG-U133 Plus 2.0 microarrays) and The



MicroRNA	P value	Fold change	locus	Expression status	Clinical value*
miR-486-3p	0.0403	6.23	8p11.21	Upregulated	ND
miR-138	0.0500	1.92	3p21.32	Upregulated	Predicts poor overall survival
miR-518b	0.0131	-65.62	19q13.42	Downregulated	-
miR-198	0.0081	-65.05	3q13.33	Downregulated	-
miR-765	0.0015	-34.02	1q23.1	Downregulated	Predicts poor overall survival
miR-222	0.0500	-5.64	Xp11.3	Downregulated	-
miR-193b	0.0418	-2.23	16p13.12	Downregulated	Predicts poor overall survival
miR-148a	0.0248	-2.15	7p15.2	Downregulated	Predicts poor overall survival
	0.0359	-2.10	1p36.13	Downregulated	-
miR-660	0.0048	-2.09	Xp11.23	Downregulated	-
miR-218	0.0048	-2.06	4p15.31	Downregulated	-

*According to Keplern meir analysis ND, no determined

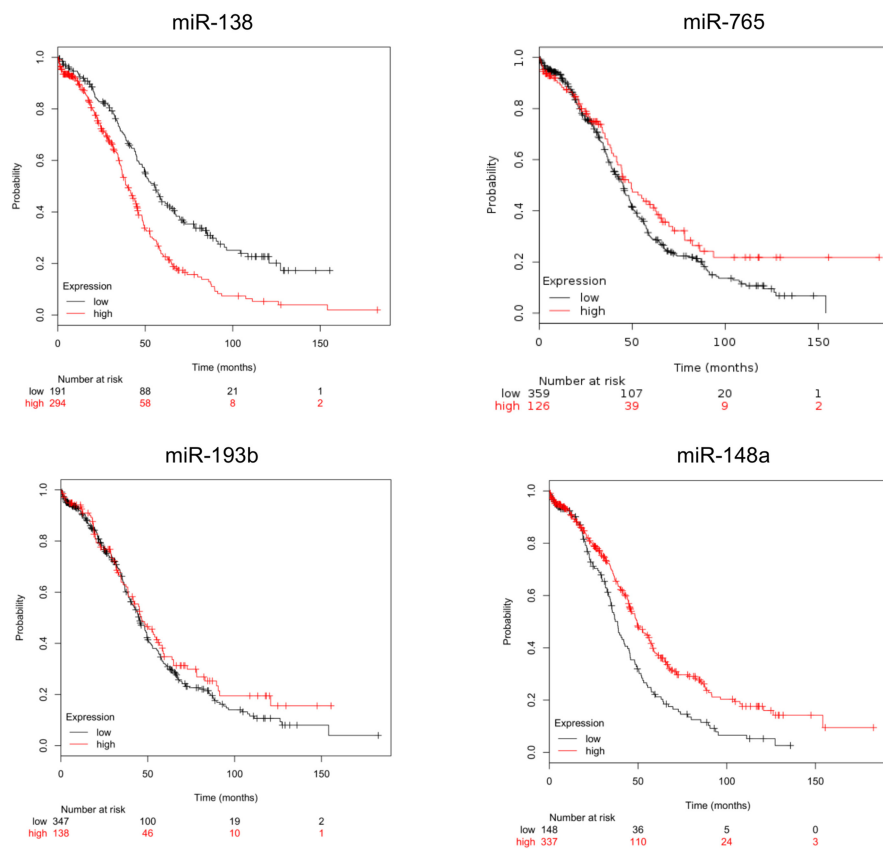


FIGURE 2 | MicroRNAs deregulated in SKOV3 cells after 48 h hypoxia. **Upper Table** illustrate the hypoxamiRs regulated in SKOV3 cells. The miRNAs expression status and clinical value predicted after Kaplan Meir analysis is depicted. **Bottom Images** showed the Kaplan Meir plots for four hypoxamiRs with potential clinical value using Start miRpower for pan-cancer as implemented in the KM plotter online tool (<http://kmplot.com/analysis/index.php?p=backgroundr>).

Cancer Genome Atlas TCGA, whereas for miRNAs expression we used Start miRpower for pan-cancer as implemented in the KM plotter at the URL (<http://kmplot.com/analysis/index.php?p=backgroundr>). To define the prognostic value of genes the samples were split into two groups according to various quantile expression of miR-765 ($n = 485$) and VEGFA, AKT1 and SRC- α genes in ovarian cancer patients ($n = 1435$). A Kaplan-Meier survival plot compared the two patient cohorts, and the hazard ratio with 95% confidence intervals and logrank P -value were calculated.

Statistical Analysis

Experiments were performed three times by triplicate and results were represented as mean \pm S.D. One-way analysis of variance (ANOVA) followed by Tukey's test were used to compare the differences between means. A $p < 0.05$ was considered as statistically significant.

RESULTS

MicroRNAs Modulated During Hypoxia-Induced 3D Channels-Like Structures Formation in Ovarian Cancer Cells

To investigate the role of hypoxia in expression of miRNAs associated with the initial phases of vasculogenic mimicry (VM), firstly we established an *in vitro* model for three-dimensional (3D) channels-like structures formation representative of the early stages of VM. We have chosen the SKOV3 ovarian cancer cells which were previously unequivocally demonstrated to form vasculogenic mimicry *in vitro* after 4 days incubation in hypoxia (19). Here, SKOV3 cells were grown in confluent monolayers

under hypoxia (1% O₂) or normoxia conditions during 48 h. Then, cells were seeding on matrigel and incubated for 0, 6, and 12 h to track the formation of 3D capillary-like structures, which represent the stages previous to VM formation. Results showed that SKOV3 cells grown in normoxia hardly exhibited the formation of cellular networks after 6 and 12 h incubation on matrigel (Figures 1A–C). When cells were grown in hypoxia, a dramatical increase in extend of cellular networks was observed during the course of time. SKOV3 cells exhibited the typical morphologic changes indicative of 3D channels-like networks formation after 0 and 6 h incubation on matrigel (Figures 1D,E). Remarkably, after 12 h incubation a significant and gradual increase in networks was found (Figure 1F). Quantification of the number of cellular networks showed that these structures were significantly augmented from 98 ± 4 to 172 ± 7 after 6 and 12 h incubation, respectively (Figure 1G). Likewise, the number of branch points was significantly increased from 43 ± 2 to 71 ± 4 after 6 and 12 h, respectively (Figure 1H). At 12 h, positive PAS staining was found mainly along the length of the cellular networks suggesting the existence of extracellular matrix compounds (Figures 1I,J). To evaluate the potential presence of tubular structures with a hollow tube, SKOV3 cells were stained with rhodamine-phalloidin and analyzed by confocal microscopy (Figures 1K,L). Immunofluorescence images of the cellular networks showed very discrete elevated structures with tubular-like appearances as observed in bright field and red channel (Figures 1M,N). A confocal microscopy Z-stack reconstruction of 12 h old 3D-cultures of SKOV3 cells hardly showed the presence of proper tubular structures with hollow centers (Figures 1N,O). These findings indicate that after 48 h hypoxia and 12 h incubation on matrigel, no clear tubules with hollow centers were generated by SKOV3 cells. Instead of

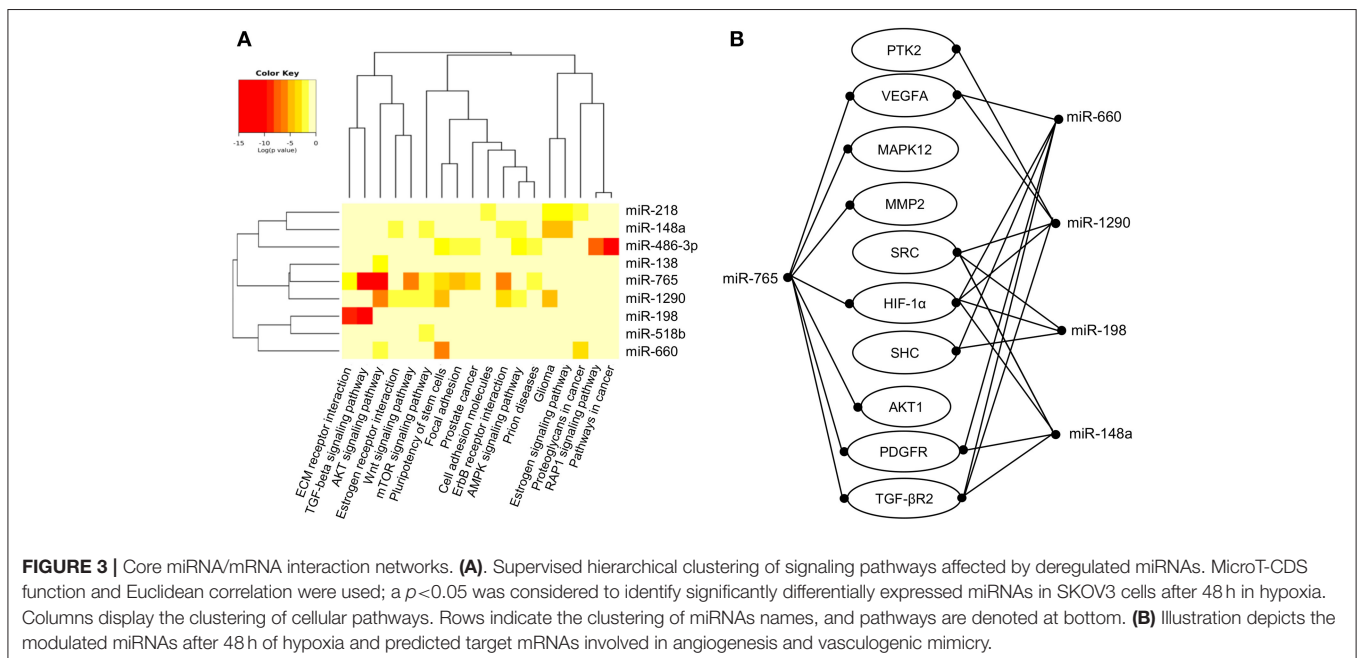


TABLE 1 | Modulated microRNAs after 48 h hypoxia in SKOV3 ovarian cancer cells and predicted targets with functions associated to cancer.

MicroRNAs	Predict target	Protein name ^a	Functions	References
UPREGULATED				
miR-486-3p	HIF1AN	Hypoxia inducible factor 1 alpha subunit inhibitor	Oxygen sensor	Kang et al. (35)
	SRCIN1	SRC kinase signaling inhibitor 1	Inhibitor of AKT/RAS pathway	
miR-138	FAM13	Fas apoptotic inhibitory molecule 3	Inhibitor of RAS pathway	Kang et al. (35)
	PTGFRN	Prostaglandin F2 receptor inhibitor	Inhibitor of angiogenesis, VM	Colin et al. (36)
	HIF1AN	Hypoxia inducible factor 1 alpha subunit inhibitor	Oxygen sensor	
DOWNREGULATED				
miR-765	VEGFA	Vascular endothelial growth factor A	Angiogenesis, proliferation, VM	Chen et al. (37)
	AKT1	RAC-alpha serine/threonine-protein kinase	Angiogenesis, proliferation, migration, VM	Rana et al. (38)
	HIF-3A	Hypoxia inducible factor 3 alpha	Angiogenesis, VM	Li et al. (39)
	PDGFR	Platelet-derived growth factor receptor	Proliferation, angiogenesis, migration	Wei et al. (40)
	TGFBR2	Transforming growth factor, beta receptor II	Proliferation, differentiation, angiogenesis, VM	Salinas-Vera et al. (6)
	MMP2	Matrix metalloproteinase 2	Angiogenesis, metastasis, VM	Ando et al. (41)
				Cuomo et al. (42)
miR-660				Avril et al. (43)
				Thijssen et al. (44)
				Plantamura et al. (45)
				Khalkhali-Ellis et al. (46)
				Kang et al. (47)
				Liang et al. (48)
	VEGFA	Vascular endothelial growth factor A	Angiogenesis, proliferation, VM	Luengo-Gil et al. (49)
	SRC	Proto-oncogene tyrosine-protein kinase	Proliferation, migration, VM	Salinas-Vera et al. (6)
	HIF-1A	Hypoxia inducible factor 1, alpha	Angiogenesis, VM	Jaraiz et al. (50)
	TGFBR2	Transforming growth factor, beta receptor II	Proliferation, differentiation, VM.	Chen et al. (37)
	PDGFR2	Platelet-derived growth factor receptor	Proliferation, differentiation, VM	Rana et al. (38)
				Plantamura et al. (45)
			Khalkhali-Ellis et al. (46)	
			Avril et al. (43)	
			Thijssen et al. (44)	
miR-218	SHC1	SHC-transforming protein 1	Proliferation, angiogenesis, VM	Salinas-Vera et al. (6)
	CDH8	Cadherin-8	Migration	Thomas et al. (51)
miR-198				Memi et al. (52)
	SRC	Proto-oncogene tyrosine-protein kinase	Proliferation, migration, VM	Salinas-Vera et al. (6)
	SHC1	SHC-transforming protein 1	Proliferation, angiogenesis, VM	Jaraiz et al. (50)
	HIF-3A	Hypoxia inducible factor 3, alpha subunit	Angiogenesis, VM	Thomas et al. (51)
	PTK2	Focal adhesion kinase 1	Proliferation, migration, VM	Suen et al. (53)
			Ando et al. (41)	
			Cuomo et al. (42)	
miR-518b	MAPK1	Mitogen-activated protein kinase 1	Angiogenesis, proliferation, VM	Wei et al. (40)
	TGFBR2	Transforming growth factor, beta receptor II	Proliferation, differentiation, angiogenesis, VM	Flum et al. (54)
			Plantamura et al. (45)	
			Khalkhali-Ellis et al. (46)	
miR-148a	TGFBR2	Transforming growth factor, beta receptor II	Proliferation, differentiation, angiogenesis, VM	Plantamura et al. (45)
	MMP16	Matrix metalloproteinase 16	Angiogenesis, metastasis	Khalkhali-Ellis et al. (46)
	HIF-3A	Hypoxia inducible factor 3 alpha subunit	Angiogenesis, VM	Kang et al. (47)
			Li et al. (55)	
			Ando et al. (41)	
			Cuomo et al. (42)	
miR-1290	VEGFA	Vascular endothelial growth factor A	Angiogenesis, proliferation, VM	Chen et al. (37)
	PTK2	Focal adhesion kinase 1	Proliferation, migration, VM	Rana et al. (38)

(Continued)

TABLE 1 | Continued

MicroRNAs	Predict target	Protein name ^a	Functions	References
	SRC	Proto-oncogene tyrosine-protein kinase	Proliferation, migration, VM	Luengo-Gil et al. (49)
	HIF-1A	Hypoxia inducible factor 1 alpha	Angiogenesis, VM	Salinas-Vera et al. (6)
	TGFBR2	Transforming growth factor, beta receptor II	Proliferation, differentiation, angiogenesis, VM	Jaraiz et al. (50)
				Chen et al. (37)
				Rana et al. (38)
				Plantamura et al. (45)
				Khalkhali-Ellis et al. (46)
miR-193b	SHC3	SHC-transforming protein 3	Proliferation, angiogenesis, VM	Liu Y et al. (56)
	GRB2	Growth factor receptor-bound protein 2	Proliferation, angiogenesis, VM	Salinas-Vera et al. (6)
	CDH4	Cadherin 4, type 1	Angiogenesis, VM	Zhang et al. (57)
	HIF3A	Hypoxia inducible factor 3 alpha subunit	Angiogenesis, VM	Xie et al. (58)
				Ando et al. (41)
				Cuomo et al. (42)
miR-222	VEGFB	Vascular endothelial growth factor B	Angiogenesis, proliferation, VM	Chen et al. (37)
	VEGFC	Vascular endothelial growth factor C	Angiogenesis, proliferation, VM	Rana et al. (38)
	SHC4	SHC-transforming protein 4	Proliferation, angiogenesis, VM	Ikeda et al. (59)
	HIF1A	Hypoxia inducible factor 1, alpha subunit	Angiogenesis, VM	Thomas et al. (51)
				Suen et al. (53)
				Chen et al. (37)
				Rana et al. (38)

^aUniprot database name; VM, vasculogenic mimicry.

we found cellular networks which were organized and lined in a time-dependent manner.

In order to identify the set of miRNAs regulated by hypoxia (hypoxamiRs) before VM formation, we profiled 667 mature miRNAs using Taq Man Low Density Arrays (TLDA) after 48 h hypoxia. Our results showed that 11 unique hypoxamiRs were significantly modulated ($FC > 1.5$; $p < 0.05$) in SKOV3 cells. Of these 9 miRNAs were downregulated (miR-765, miR-660, miR-218, miR-198, miR-518b, miR-148a, miR-1290, miR-193b, miR-222) and 2 upregulated (miR-486-3p, miR-138) in comparison to control cells grown without hypoxia (time 0) (Figure 2). Next, we were wondering if expression levels of the set of modulated miRNAs may have clinical implications in ovarian cancer. Therefore, we performed overall survival analysis using Kaplan Meier tool (Start miRpower pan-cancer) which utilize genome-wide transcriptome data and overall survival clinical information from a large cohort of ovarian cancer patients ($n = 485$) with a follow-up of 180 months as described in material and methods (33, 34). To define the prognostic value of genes the samples were split into two groups according to quantile expression of miRNAs. A Kaplan-Meier survival plot compared the two patient cohorts, and the hazard ratio with 95% confidence intervals and logrank P -value were calculated. Results showed that high expression of miR-138 ($HR = 1.80$, logrank $P = 5.3e-07$) and low levels of miR-765 ($HR = 0.77$, logrank $P = 0.05$), miR-193b ($HR = 0.86$, logrank $P = 0.25$), and miR-148a ($HR = 0.63$, logrank $P = 0.0001$) genes were associated to low overall survival of ovarian cancer patients (Figure 2).

HypoxamiRs Regulate Cellular Pathways Associated With Cancer

Predictive analysis of the set of regulated hypoxamiRs suggested that they might impact common cellular processes and signaling pathways related with tumorigenesis (Figure 3A). The signaling pathways enriched were TGF- β , WNT, mTOR, AMPK, estrogen receptor and RAP1. Computational predictions also indicated that these miRNAs may target a number of genes involved in VM and angiogenesis including HIF-1A, HIF-1AN, HIF-3A, PTGFRN, AKT1, VEGFA, VEGFB, VEGFC, PDGFR, TGF- β 2, MMP2, PTK2, SRC, SHC3, and GRB2, among others (Table 1). In particular, we focused in miR-765 for further functional analysis because: (i) it was severely downregulated after hypoxia ($FC < 32.02$; $p < 0.05$), (ii) it was predicted to target a number of genes involved in VM (Figure 3B), and (iii) there is no reports about the functions of miR-765 in ovarian cancer neither in tumor VM.

Hypoxia-Suppressed miR-765 Inhibits Channels-Like Networks Formation

To examine the functional role of miR-765 on 3D channels-like networks, we restored its expression in SKOV3 cells by transfection of specific RNA mimics. Then, 3D channels-like networks formation was induced by 48 h hypoxia as described before. Non-transfected and scramble-treated cells were included as controls. Interestingly, ectopic restoration of miR-765 produced a dramatic inhibition of 3D channels-like networks formation (Figure 4A). A significant reduction

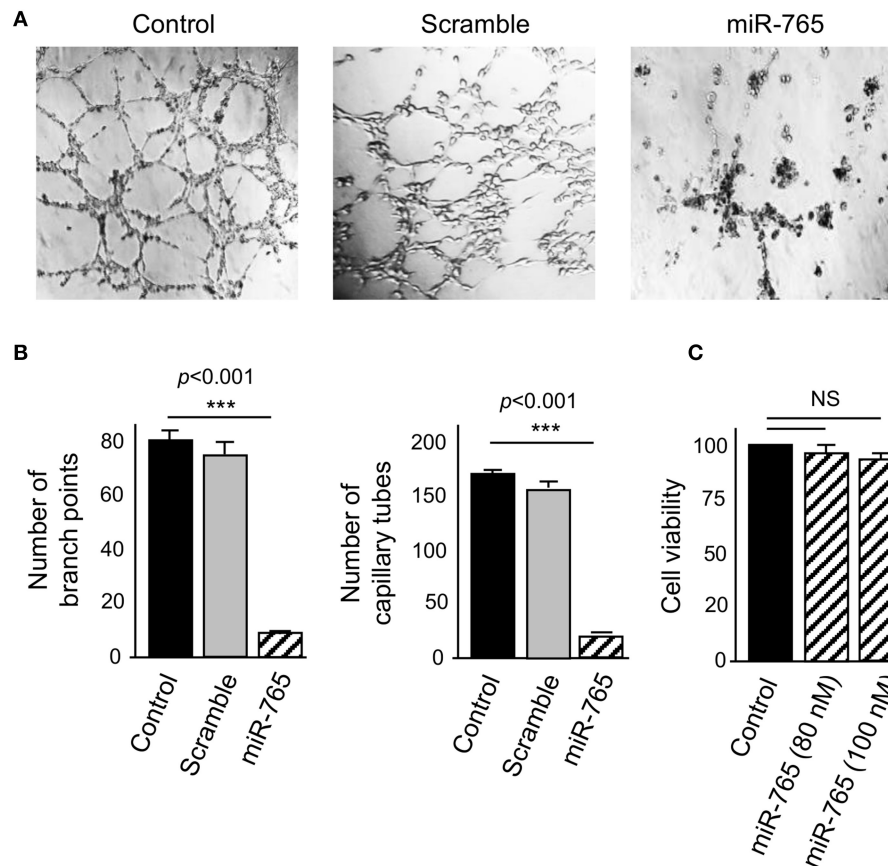


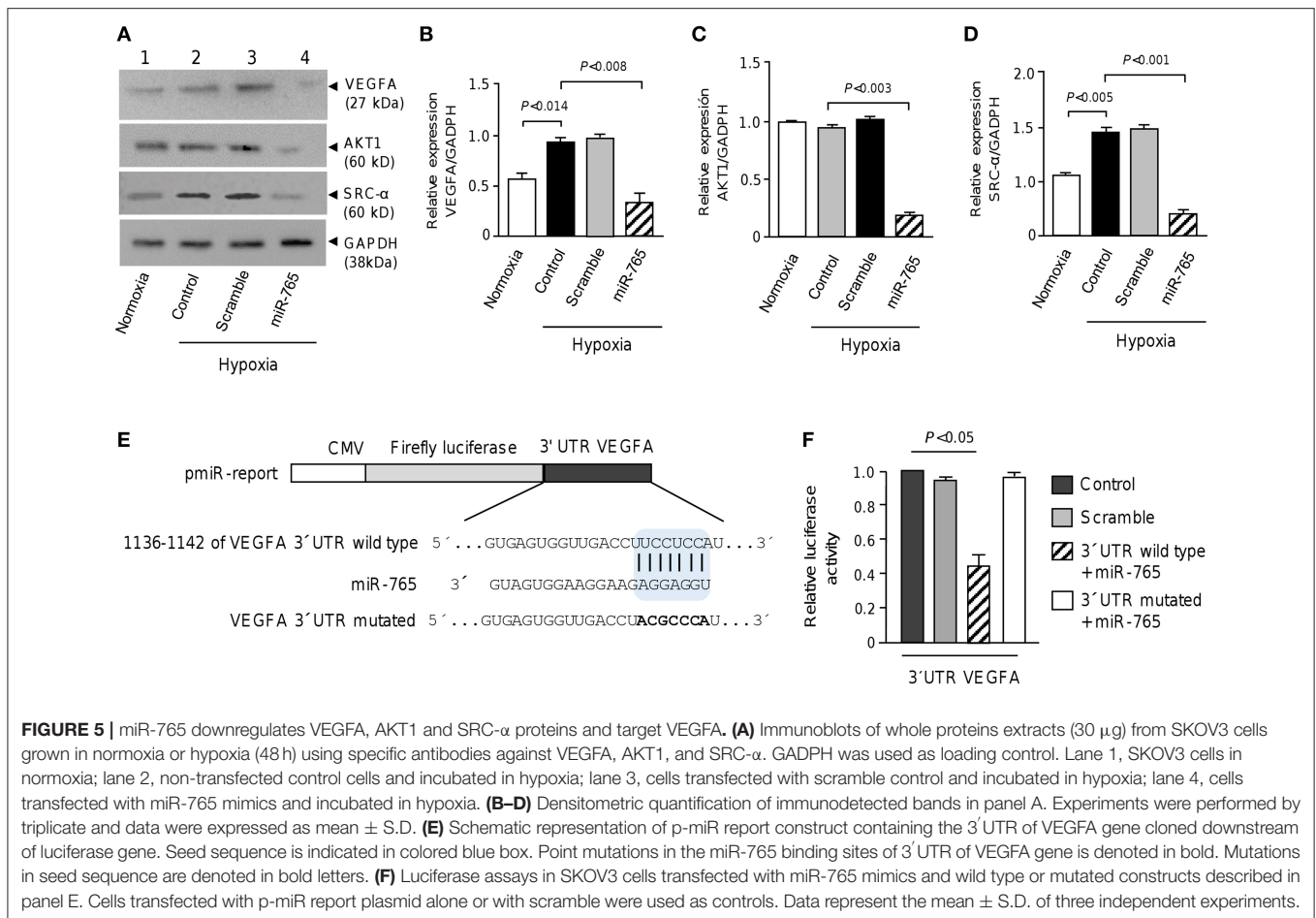
FIGURE 4 | miR-765 inhibits hypoxia-induced 3D channels-like structures. **(A)** 3D channels-like structures of SKOV3 cells transfected with miR-765 mimics (right panel), scramble (middle panel) and no-transfected control cells (left panel) and grown for 48 h in hypoxia and then 12 h in matrigel. **(B)** Graphical representation of the number of branch points and capillary-like channels from **(A)**. **(C)** Cell viability assays of SKOV3 cells transfected with increasing concentrations of miR-765. Experiments were performed by three times by triplicate and data were expressed as mean \pm S.D. *** $p < 0.001$. NS, non-significant.

of the number of branch points (up to 85%) and capillary tubes (up to 92%) were found in miR-765-transfected cells in comparison to control cells (**Figure 4B**). To discard pleiotropic effects of miR-765 overexpression in cell survival of ovarian cancer cells, we performed cell viability assays. Data showed no significant changes in viability of miR-765-expressing SKOV3 cancer cells at the tested concentrations which indicate that the effect of miR-765 in 3D channels-like networks impairment was specific (**Figure 4C**).

MiR-765 Downregulates VEGFA, AKT1 and SRC- α and Directly Target VEGFA

Because the bioinformatics predictions of gene targets suggested that several signaling pathways such as VEGFA, AKT, and SRC/FAK, could be affected in SKOV3 cells transfected with miR-765, we proceed to evaluate the changes in expression of the aforementioned proteins using available antibodies in Western blot assays (**Figure 5**). Results showed that VEGFA protein was expressed at low levels in cells cultured under normoxia conditions, but its expression was significantly increased under hypoxia. Moreover, we observed a significant decrease in VEGFA

levels in SKOV3 cells transfected with miR-765 mimics in comparison to non-treated and scramble transfected controls cells (**Figures 5A,B**). Likewise, a significant decrease in both SRC- α and AKT1 levels was found in cells transfected with miR-765 mimics in comparison to control cells (**Figures 5A,C,D**). No significant changes were observed in GADPH levels used as control. Computational predictions also showed that miR-765 may target a number of protein-encoding genes with known roles in VM. Of these, we focused in the study of VEGFA as it was downregulated by miR-765 and it contain a potential miR-765 binding site at 3'UTR (**Figure 5E**). To corroborate whether miR-765 can exert posttranscriptional repression of VEGFA, we performed luciferase reporter assays. A DNA fragment corresponding to 3'UTR of VEGFA was cloned downstream of the luciferase-coding region of pmiR-LUC vector (**Figure 5E**). In addition, a mutated version of the miR-765 binding site at the VEGFA 3'UTR was included as a plasmid control. Data showed that ectopic expression of miR-765 and co-transfection of recombinant VEGFA 3'UTR wild type plasmid into SKOV3 cells resulted in a significant reduction of the relative luciferase activity in comparison with



controls (**Figure 5B**). In addition, when mutated sequence was assayed no significant changes in luciferase activity were found. Altogether these data confirmed that VEGFA is a novel target of miR-765.

Expression Levels of miR-765, VEGFA, AKT1, and SRC- α Correlate With Poor Patient's Outcome

Then we were wondering if changes in expression levels of miR-765, VEGFA, AKT1 and SRC- α have clinical implications in ovarian cancer. Thus, we performed overall survival analysis using Start Kaplan Meier plotter for ovarian cancer which use genome-wide transcriptome data and overall survival clinical information from a large cohort of ovarian cancer patients ($n = 1485$) with a mean follow-up of 170 months. To define the prognostic value of genes the samples were split into two groups according to various quantile expression of VEGFA, AKT1 and SRC- α genes. A Kaplan-Meier survival plot compared the two patient cohorts, and the hazard ratio with 95% confidence intervals and logrank P -value were calculated. Results showed that low levels of miR-765 (HR = 0.77, logrank $P = 0.05$) and high expression of its targets VEGFA (HR = 1.38, logrank $P = 1.8e-05$), AKT1 (HR = 1.19, logrank $P =$

0.0071), and SRC- α (HR = 1.39, logrank $P = 0.000092$) signaling genes were associated to low overall survival of ovarian cancer patients (**Figure 6**).

DISCUSSION

Tumor VM is a highly orchestrated cellular mechanism in which highly aggressive and metastatic tumor cells form vascular-like 3D networks to provide an efficient and functional fluid-conducting system for blood and oxygen supply, as an alternative to classical vasculogenesis. This morphologic plasticity is associated to high aggressiveness, increased metastasis and tumor progression of certain types of cancers. In clinical VM has been related with low overall survival and resistance to current anti-angiogenic therapies (60). Remarkably, tumor VM can be potentially targeted by novel therapeutic agents, thus currently diverse investigations in the search of novel VM regulators are undergoing. In order to contribute with the understanding of the role of small non-coding RNAs in the molecular mechanisms responsible for VM, here we have uncovered a novel set of miRNAs modulated at the early onset of hypoxia-induced 3D channels-like structures formation, previous to the proper formation of tubules indicative of VM in SKOV3 cells. We first

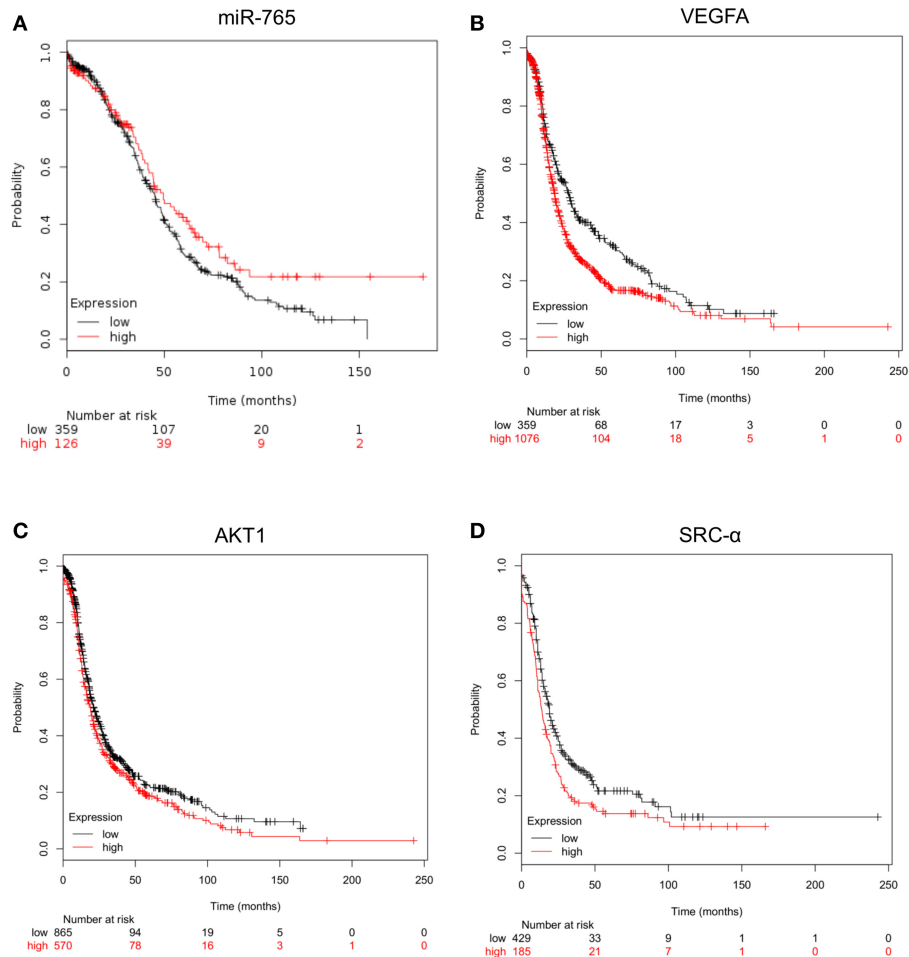


FIGURE 6 | Kaplan-Meier curves for overall survival according to the expression of miR-765, VEGFA, AKT1 and SRC- α . Overall survival analysis using Kaplan Meier plotter for **(A)** miR-765, **(B)** VEGFA, **(C)** AKT1, and **(D)** SRC- α genes. Start KM plotter for ovarian cancer tool used genome-wide for mRNA expression data and overall survival clinical information of cancer patients, which were downloaded from Gene Expression Omnibus GEO (Affymetrix HG-U133A, HG-U133A 2.0, and HG-U133 plus 2.0 microarrays) and The Cancer Genome Atlas TCGA, whereas for miRNAs expression we used Start miRpower for pan-cancer as implemented in the KM plotter. Samples were split into two groups according to various quantile expression of miR-765 ($n = 485$) and VEGFA, AKT1 and SRC- α genes in ovarian cancer patients ($n = 1435$). Kaplan-Meier survival plots compared the two patient cohorts, and the hazard ratio with 95% confidence intervals and logrank P -value were calculated.

set-up an *in vitro* model, and using PAS staining we confirmed that SKOV3 cells efficiently form 3D channels-like networks in agreement with other studies (16, 61–63). It's important to note that the tubular-like structures we have analyzed here, may not reflect VM properly, but they represents the early stages of VM and the morphological and transcriptional programs activated by 48 h hypoxia, previous to VM appearance. It's important to remarks the urgency of confirmatory *in vitro* assays for proper VM in the different types of cancer, as a recent report (19) surprisingly suggested that many of structures reported in the literature at early times of hypoxia may not represent VM, as we can confirm in the present study.

Hypoxia is an important activator of VM, thus we decided to search for the miRNAs regulated by hypoxia (hypoxamiRs) during initial stages of VM, as it remains largely unknown in ovarian cancer. Our results showed that 11 hypoxamiRs

were significantly modulated. Of these 9 miRNAs were downregulated (miR-765, miR-660, miR-218, miR-198, miR-518b, miR-148a, miR-1290, miR-193b, miR-222) and 2 upregulated (miR-486-3p, miR-138) (Figure 2). Interestingly, high expression of miR-138 and low levels of miR-765, miR-193b, and miR-148a genes were associated to low overall survival suggesting a potential clinical value in ovarian cancer patients (Figure 2). However, we cannot drawn a solid connection between outcome and VM in patients, as we have collected the clinical data from KMplot databases, and unfortunately no VM presence/absence data is available for the cohort of patients analyzed here. Thus, we have limited the conclusions only to a correlation between miRNAs regulated by hypoxia and the overall survival. On the other hand, several of the regulated miRNAs have been previously associated with tumorigenesis in diverse types of cancer. For instance, miR-660 was reported as

downregulated in lung cancer patients and its transient and stable overexpression using RNA mimics reduced migration, invasion, and proliferation properties and increased apoptosis in p53 wild-type lung cancer cells (64). Likewise, miR-218-5p expression was lower in cervical cancer tumors in comparison with normal tissues. MiR-218-5p suppressed the progression of cervical cancer via *LYN/NF-κB* signaling pathway (65). In addition, miR-138 promotes cell proliferation and invasion on colorectal cancer (66), and it contributes to resistance to therapy in multiple myeloma and non-small cell lung cancer (67, 68). Of the set of regulated hypoxamiRs, we focused in the study of functional relationships between miR-765 and 3D channels-like formation. Recently, miR-765 have been reported as upregulated or downregulated in diverse types of malignancies such as esophageal squamous cell carcinoma (69), melanoma (70), osteosarcoma (71), oral squamous cancer (72) and hepatocellular carcinoma (73). Nevertheless, miR-765 functions in ovarian cancer and tumor VM remains largely unknown. Our data showed that the ability of SKOV3 cells to develop 3D channels-like structures formation under hypoxia was significantly reduced after transfection of miR-765 mimics. This may be explained as the target predictions indicate that miR-765 may regulate genes associated to the cell proliferation, matrix remodeling, migration, and invasion, angiogenesis, and VM formation. Indeed, we demonstrated that miR-765 was able to downregulate the VEGFA, AKT1 and SRC-α signaling transducer critical in VM. Also important is the fact that expression of miR-765 and its aforementioned gene targets have a potential clinical value as its deregulation was associated with worst outcome in ovarian cancer patients (Figure 6). Main limitations of the present study are denoted by the use of a single cell model, which however, permit us to delineate important conclusions about the hypoxamiRs modulated in SKOV3 cells, and guide us to the analysis of miR-765 and its role in 3D channels-like structures formation.

REFERENCES

- Maniotis AJ, Folberg R, Hess A, Sefter EA, Gardner LM, Pe'er J, et al. Vascular channel formation by human melanoma cells *in vivo* and *in vitro*: vasculogenic mimicry. *Am J Pathol.* (1999) 155:739–52. doi: 10.1016/S0002-9440(10)65173-5
- Hendrix MJ, Sefter EA, Hess AR, Sefter RE. Vasculogenic mimicry and tumour-cell plasticity: lessons from melanoma. *Nat Rev Cancer.* (2003) 3:411–21. doi: 10.1038/nrc1092
- Shirakawa K, Kobayashi H, Heike Y, Kawamoto S, Brechbiel MW, Kasumi F, et al. Hemodynamics in vasculogenic mimicry and angiogenesis of inflammatory breast cancer xenograft. *Cancer Res.* (2002) 15:560–6.
- El Hallani S, Boisselier B, Peglion F, Rousseau A, Colin C, Idhahbi A, et al. A new alternative mechanism in glioblastoma vascularization: tubular vasculogenic mimicry. *Brain.* (2010) 133:973–82. doi: 10.1093/brain/awq044
- Basu GD, Liang WS, Stephan DA, Wegener LT, Conley CR, Pockaj BA, et al. A novel role for cyclooxygenase-2 in regulating vascular channel formation by human breast cancer cells. *Breast Cancer Res.* (2006) 8:R69. doi: 10.1186/bcr1626
- Salinas-Vera YM, Marchat LA, García-Vázquez R, González de la Rosa CH, Castañeda-Saucedo E, Tito NN, et al. Cooperative multi-targeting of signaling networks by angiomiR-204 inhibits vasculogenic mimicry in breast cancer cells. *Cancer Lett.* (2018) 28, 17–27. doi: 10.1016/j.canlet.2018.06.003

Nonetheless, we understand the need to extend our initial findings in additional ovarian cancer cell lines in future studies. Also, a limitation of the present study is that we specifically analyzed here the early stages of VM (after 48 h hypoxia); thus the potential role of the revealed miRNAs signature at later stages of proper VM is unknown. Taken altogether, we propose that miR-765 may regulate 3D channels-like structures formation through both direct and indirect targeting of signaling transducers. Also, we suggested that miR-765 could impair VEGFA by direct binding to VEGFA and AKT1; as well as by indirect downregulation of SRC-α which in turn may block the VEGFA/AKT1 signaling transduction. In conclusion, in the current work we provide a novel set of regulated hypoxamiRs and experimental data supporting an unexpected role for VEGFA/AKT1/SRC-α axis in 3D channels-like structures formation in SKOV3 cells. As novel therapies targeting hypoxic cancer cells are needed to improve therapy treatment of cancer, we consider that our data are relevant and deserves further *in vivo* validation.

AUTHOR CONTRIBUTIONS

YS-V, RG-V, OH, EC-S, and MR-H conducted all the experiments. JG-B performed the microRNAs profiling. CV-C performed the confocal microscopy. JC-C provide advice in cell cultures. DG-R, ER-G, HA, and AC-P contributed to experimental design, intellectual input, and interpreting data. CL-C and LM wrote the manuscript.

ACKNOWLEDGMENTS

The authors acknowledge the Grupo Mexicano de Investigación en Cáncer de Ovario for research funding and support. The authors also acknowledge the Universidad Autónoma de la Ciudad de Mexico for support.

- Sharma N, Sefter RE, Sefter EA, Gruman LM, Heidger PM Jr., Cohen MB, et al. Prostatic tumor cell plasticity involves cooperative interactions of distinct phenotypic subpopulations: role in vasculogenic mimicry. *Prostate.* (2002) 15:189–201. doi: 10.1002/pros.10048
- Williamson SC, Metcalf RL, Trapani F, Mohan S, Antonello J, Abbott B, et al. Vasculogenic mimicry in small cell lung cancer. *Nat Commun.* (2016) 9:13322. doi: 10.1038/ncomms13322
- Sun B, Zhang S, Zhang D, Du J, Guo H, Zhao X, et al. Vasculogenic mimicry is associated with high tumor grade, invasion and metastasis, and short survival in patients with hepatocellular carcinoma. *Oncol Rep.* (2006) 16:693–8. doi: 10.3892/or.16.4.693
- Du J, Sun B, Zhao X, Gu Q, Dong X, Mo J, et al. Hypoxia promotes vasculogenic mimicry formation by inducing epithelial-mesenchymal transition in ovarian carcinoma. *Gynecol Oncol.* (2014) 133:575–83. doi: 10.1016/j.ygyno.2014.02.034
- Sood AK, Fletcher MS, Zahn CM, Gruman LM, Coffin JE, Sefter EA, et al. The clinical significance of tumor cell-lined vasculature in ovarian carcinoma: implications for anti-vasculogenic therapy. *Cancer Biol Ther.* (2002) 1:661–4. doi: 10.4161/cbt.316
- Cao Z, Bao M, Miele L, Sarkar FH, Wang Z, Zhou Q. Tumour vasculogenic mimicry is associated with poor prognosis of human cancer patients: a systemic review and meta-analysis. *Eur J Cancer.* (2013) 49:3914–23. doi: 10.1016/j.ejca.2013.07.148

13. Jain RK, Duda DG, Willett CG, Sahani DV, Zhu AX, Loeffler JS, et al. Biomarkers of response and resistance to antiangiogenic therapy. *Nat Rev Clin Oncol.* (2009) 6:327–38. doi: 10.1038/nrclinonc.2009.63
14. Pinto MP, Sotomayor P, Carrasco-Avino G, Corvalan AH, Owen GI. Escaping antiangiogenic therapy: strategies employed by cancer cells. *Int J Mol Sci.* (2016) 6:E1489. doi: 10.3390/ijms17091489
15. Ge H, Luo H. Overview of advances in vasculogenic mimicry - a potential target for tumor therapy. *Cancer Manag Res.* (2018) 2:2429–37. doi: 10.2147/CMAR.S164675
16. Sood AK, Seftor EA, Fletcher MS, Gardner LM, Heidger PM, Buller RE, et al. Molecular determinants of ovarian cancer plasticity. *Am J Pathol.* (2001) 158:1279–88. doi: 10.1016/S0002-9440(10)64079-5
17. Maniotis AJ, Chen X, Garcia C, DeChristopher PJ, Wu D, Pe'er J, et al. Control of melanoma morphogenesis, endothelial survival, and perfusion by extracellular matrix. *Lab Invest.* (2002) 82:1031–43. doi: 10.1097/01.LAB.0000024362.12721.67
18. Hess AR, Seftor EA, Gardner LM, Carles-Kinch K, Schneider GB, Seftor RE, et al. Molecular regulation of tumor cell vasculogenic mimicry by tyrosine phosphorylation: role of epithelial cell kinase (Eck/EphA2). *Cancer Res.* (2001) 15:3250–5.
19. Racordon D, Valdivia A, Mingo G, Erices R, Aravena R, Santoro F, et al. Structural and functional identification of vasculogenic mimicry *in vitro*. *Sci Rep.* (2017) 7:6985. doi: 10.1038/s41598-017-07622-w
20. Demou ZN. Time-lapse analysis and microdissection of living 3D melanoma cell cultures for genomics and proteomics. *Biotechnol Bioeng.* (2008) 101:307–16. doi: 10.1002/bit.21899
21. Hendrix MJ, Seftor EA, Meltzer PS, Gardner LM, Hess AR, Kirschmann DA, et al. Expression and functional significance of VE-cadherin in aggressive human melanoma cells: role in vasculogenic mimicry. *Proc Natl Acad Sci USA.* (2001) 98:8018–23. doi: 10.1073/pnas.131209798
22. Fan YZ, Sun W. Molecular regulation of vasculogenic mimicry in tumors and potential tumor-target therapy. *World J Gastrointest Surg.* (2010) 27:117–27. doi: 10.4240/wjgs.v2.i4.117
23. Kirschmann DA, Seftor EA, Hardy KM, Seftor RE, Hendrix MJ. Molecular pathways: vasculogenic mimicry in tumor cells: diagnostic and therapeutic implications. *Clin Cancer Res.* (2012) 15:2726–32. doi: 10.1158/1078-0432.CCR-11-3237
24. Paulis YW, Soetekouw PM, Verheul HM, Tjan-Heijnen VC, Griffioen AW. Signalling pathways in vasculogenic mimicry. *Biochim Biophys Acta.* (2010) 1806:18–28. doi: 10.1016/j.bbcan.2010.01.001
25. Qiao L, Liang N, Zhang J, Xie J, Liu F, Xu D, et al. Advanced research on vasculogenic mimicry in cancer. *J Cell Mol Med.* (2015) 19:315–26. doi: 10.1111/jcmm.12496
26. Li S, Meng W, Guan Z, Guo Y, Han X. The hypoxia-related signaling pathways of vasculogenic mimicry in tumor treatment. *Biomed Pharmacother.* (2016) 80:127–35. doi: 10.1016/j.biopha.2016.03.010
27. Hess AR, Seftor EA, Gruman LM, Kinch MS, Seftor RE, Hendrix MJ. VE-cadherin regulates EphA2 in aggressive melanoma cells through a novel signaling pathway: implications for vasculogenic mimicry. *Cancer Biol Ther.* (2006) 5:228–33. doi: 10.4161/cbt.5.2.2510
28. Calin GA, Croce CM. MicroRNA signatures in human cancers. *Nat Rev Cancer.* (2006) 6:857–66. doi: 10.1038/nrc3932
29. Lin S, Gregory RI. MicroRNA biogenesis pathways in cancer. *Nat Rev Cancer.* (2015) 15:321–33. doi: 10.1038/nrc3932
30. Wu N, Zhao X, Liu M, Liu H, Yao W, Zhang Y, et al. Role of microRNA-26b in glioma development and its mediated regulation on EphA2. *PLoS ONE.* (2011) 14:e16264. doi: 10.1371/journal.pone.0016264
31. Sun Q, Zou X, Zhang T, Shen J, Yin Y, Xiang J. The role of miR-200a in vasculogenic mimicry and its clinical significance in ovarian cancer. *Gynecol Oncol.* (2014) 132:730–8. doi: 10.1016/j.ygyno.2014.01.047
32. Liu W, Lv C, Zhang B, Zhou Q, Cao Z. MicroRNA-27b functions as a new inhibitor of ovarian cancer-mediated vasculogenic mimicry through suppression of VE-cadherin expression. *RNA.* (2017) 23:1019–27. doi: 10.1261/rna.059592.116
33. Gyorffy B, Lániczky A, Szállási Z. Implementing an online tool for genome-wide validation of survival-associated biomarkers in ovarian-cancer using microarray data from 1287 patients. *Endocr Relat Cancer.* (2012) 10:197–208. doi: 10.1530/ERC-11-0329
34. Nagy Á, Lániczky A, Menyhárt O, Gyorffy B. Validation of miRNA prognostic power in hepatocellular carcinoma using expression data of independent datasets. *Sci Rep.* (2018) 8:9277. doi: 10.1038/s41598-018-29514-3
35. Kang J, Shin SH, Yoon H, Huh J, Shin HW, Chun YS, et al. FIH is an oxygen sensor in ovarian cancer for G9a/GLP-driven epigenetic regulation of metastasis-related genes. *Cancer Res.* (2017) 78:1184–19. doi: 10.1158/0008-5472.CAN-17-2506
36. Colin S, Guilmain W, Creoff E, Schneider C, Steverlynck C, Bongaerts M, et al. A truncated form of CD9-partner 1 (CD9P-1), GS-168AT2, potently inhibits *in vivo* tumour-induced angiogenesis and tumour growth. *Br J Cancer.* (2011) 105:1002–11. doi: 10.1038/bjc.2011.303
37. Chen Y, Zhang L, Liu WX, Wang K. VEGF and SEMA4D have synergistic effects on the promotion of angiogenesis in epithelial ovarian cancer. *Cell Mol Biol Lett.* (2018) 323:22. doi: 10.1186/s11658-017-0058-9
38. Rana NK, Singh P, Koch B. CoCl₂ simulated hypoxia induce cell proliferation and alter the expression pattern of hypoxia associated genes involved in angiogenesis and apoptosis. *Biol Res.* (2019) 52:12. doi: 10.1186/s40659-019-0221-z
39. Li Y, Sun B, Zhao X, Wang X, Zhang D, Gu Q, et al. MMP-2 and MMP-13 affect vasculogenic mimicry formation in large cell lung cancer. *J Cell Mol Med.* (2017) 21:3741–51. doi: 10.1111/jcmm.13283
40. Wei WT, Nian XX, Wang SY, Jiao HL, Wang YX, Xiao ZY, Yang R. miR-422a inhibits cell proliferation in colorectal cancer by targeting AKT1 and MAPK1. *Cancer Cell Int.* (2017) 28:91. doi: 10.1186/s12935-017-0461-3
41. Ando H, Natsume A, Iwami K, Ohka F, Kuchimaru T, Kizaka-Kondoh S, et al. A hypoxia-inducible factor (HIF)-3 α splicing variant, HIF-3 α 4 impairs angiogenesis in hypervascular malignant meningiomas with epigenetically silenced HIF-3 α 4. *Biochem Biophys Res Commun.* (2013) 433:139–44. doi: 10.1016/j.bbrc.2013.02.044
42. Cuomo F, Coppola A, Botti C, Maione C, Forte A, Scisciola L, et al. Pro-inflammatory cytokines activate hypoxia-inducible factor 3 α via epigenetic changes in mesenchymal stromal/stem cells. *Sci Rep.* (2018) 8:5842. doi: 10.1038/s41598-018-24221-5
43. Avril S, Dincer Y, Malinowsky K, Wolff C, Gündisch S, Hapfelmeier A. Increased PDGFR-beta and VEGFR-2 protein levels are associated with resistance to platinum-based chemotherapy and adverse outcome of ovarian cancer patients. *Oncotarget.* (2017) 8:97851–61. doi: 10.18632/oncotarget.18415
44. Thijssen VL, Paulis YW, Nowak-Sliwinska P, Deumelandt KL, Hosaka K, Soetekouw PM, et al. Targeting PDGF-mediated recruitment of pericytes blocks vascular mimicry and tumor growth. *J Pathol.* (2018) 246:447–58. doi: 10.1002/path.5152
45. Plantamura I, Casalini P, Dugnani E, Sasso M, D'Ippolito E, Tortoreto M, et al. PDGFR β and FGFR2 mediate endothelial cell differentiation capability of triple negative breast carcinoma cells. *Mol Oncol.* (2014) 8:968–81. doi: 10.1016/j.molonc.2014.03.015
46. Khalkhali-Ellis Z, Kirschmann DA, Seftor EA, Gilgur A, Bodenstein TM, Hinck AP, et al. Divergence(s) in nodal signaling between aggressive melanoma and embryonic stem cells. *Int J Cancer.* (2015) 136:E242–51. doi: 10.1002/ijc.29198
47. Kang DY, Sp N, Kim DH, Joung YH, Lee HG, Park YM, et al. Salidroside inhibits migration, invasion and angiogenesis of MDA-MB 231 TNBC cells by regulating EGFR/Jak2/STAT3 signaling via MMP2. *Int J Oncol.* (2018) 53:877–85. doi: 10.3892/ijo.2018.4430
48. Liang X, Sun R, Zhao X, Zhang Y, Gu Q, Dong X, et al. Rictor regulates the vasculogenic mimicry of melanoma via the AKT-MMP-2/9 pathway. *J Cell Mol Med.* (2017) 21:3579–91. doi: 10.1111/jcmm.13268
49. Luengo-Gil G, Gonzalez-Billalabeitia E, Perez-Henarejos SA, Navarro Manzano E, Chaves-Benito A, Garcia-Martinez E. Angiogenic role of miR-20a in breast cancer. *PLoS ONE.* (2018) 13:e0194638. doi: 10.1371/journal.pone.0194638
50. Jaraíz-Rodríguez M, Tabernero MD, González-Tablas M, Otero A, Orfao A, Medina JM, et al. A short region of connexin43 reduces human glioma stem cell migration, invasion, and survival through Src, PTEN, and FAK. *Stem Cell Rep.* (2017) 9:451–63. doi: 10.1016/j.stemcr.2017.06.007
51. Thomas SL, Alam R, Lemke N, Schultz LR, Gutiérrez JA, Rempel SA. PTEN augments SPARC suppression of proliferation and inhibits SPARC-induced

- migration by suppressing SHC-RAF-ERK and AKT signaling. *Neuro Oncol.* (2010) 12:941–55. doi: 10.1093/neuonc/noq048
52. Memi F, Killen AC, Barber M, Parnavelas JG, Andrews WD. Cadherin 8 regulates proliferation of cortical interneuron progenitors. *Brain Struct Funct.* (2019) 224:277–92. doi: 10.1007/s00429-018-1772-4
 53. Suen KM, Lin CC, Seiler C, George R, Poncet-Montange G, Biter AB, et al. Phosphorylation of threonine residues on Shc promotes ligand binding and mediates crosstalk between MAPK and Akt pathways in breast cancer cells. *Int J Biochem Cell Biol.* (2018) 94:89–97. doi: 10.1016/j.biocel.2017.11.014
 54. Flum M, Kleemann M, Schneider H, Weis B, Fischer S, Handrick R, et al. miR-217-5p induces apoptosis by directly targeting PRKCI, BAG3, ITGAV and MAPK1 in colorectal cancer cells. *J Cell Commun Signal.* (2018) 12:451–66. doi: 10.1007/s12079-017-0410-x
 55. Li CH, Sun XJ, Niu SS, Yang CY, Hao YP, Kou JT, et al. Overexpression of IQGAP1 promotes the angiogenesis of esophageal squamous cell carcinoma through the AKT and ERK-mediated VEGF-VEGFR2 signaling pathway. *Oncol Rep.* (2018) 40:1795–802. doi: 10.3892/or.2018.6558
 56. Liu Y, Zhang X, Yang B, Zhuang H, Guo H, Wei W, et al. Demethylation-Induced Overexpression of Shc3 Drives c-Raf-Independent Activation of MEK/ERK in HCC. *Cancer Res.* (2018) 78:2219–32. doi: 10.1158/0008-5472.CAN-17-2432
 57. Zhang Y, Xu G, Liu G, Ye Y, Zhang C, Fan C, et al. miR-411-5p inhibits proliferation and metastasis of breast cancer cell via targeting GRB2. *Biochem Biophys Res Commun.* (2016) 476:607–13. doi: 10.1016/j.bbrc.2016.06.006
 58. Xie J, Feng Y, Lin T, Huang XY, Gan RH, Zhao Y, et al. CDH4 suppresses the progression of salivary adenoid cystic carcinoma via E-cadherin co-expression. *Oncotarget.* (2016) 7:82961–71. doi: 10.18632/oncotarget.12821
 59. Ikeda K, Oki E, Saeki H, Ando K, Morita M, Oda Y, et al. Intratumoral lymphangiogenesis and prognostic significance of VEGFC expression in gastric cancer. *Anticancer Res.* (2014) 34:3911–5.
 60. Xu Y, Li Q, Li XY, Yang QY, Xu WW, Liu GL. Short-term anti-vascular endothelial growth factor treatment elicits vasculogenic mimicry formation of tumors to accelerate metastasis. *J Exp Clin Cancer Res.* (2012) 23:16. doi: 10.1186/1756-9966-31-16
 61. Wang JY, Sun T, Zhao XL, Zhang SW, Zhang DF, Gu Q, et al. Functional significance of VEGF-a in human ovarian carcinoma: role in vasculogenic mimicry. *Cancer Biol Ther.* (2008) 7:758–66. doi: 10.4161/cbt.7.5.5765
 62. Millimaggi D, Mari M, D'Ascenzo S, Giusti I, Pavan A, Dolo V. Vasculogenic mimicry of human ovarian cancer cells: role of CD147. *Int J Oncol.* (2009) 35:1423–8. doi: 10.3892/ijo_00000460
 63. Zhu P, Ning Y, Yao L, Chen M, Xu C. The proliferation, apoptosis, invasion of endothelial-like epithelial ovarian cancer cells induced by hypoxia. *J Exp Clin Cancer Res.* (2010) 10:124. doi: 10.1186/1756-9966-29-124
 64. Fortunato O, Boeri M, Moro M, Verri C, Mensah M, Conte D, et al. Mir-660 is downregulated in lung cancer patients and its replacement inhibits lung tumorigenesis by targeting MDM2-p53 interaction. *Cell Death Dis.* (2014) 11:e1564. doi: 10.1038/cddis.2014.507
 65. Xu Y, He Q, Lu Y, Tao F, Zhao L, Ou R. MicroRNA-218-5p inhibits cell growth and metastasis in cervical cancer via LYN/NF- κ B signaling pathway. *Cancer Cell Int.* (2018) 4:198. doi: 10.1186/s12935-018-0673-1
 66. Xu Y, Pan ZG, Shu L, Li QJ. Podocalyxin-like, targeted by miR-138, promotes colorectal cancer cell proliferation, migration, invasion and EMT. *Eur Rev Med Pharmacol Sci.* (2018) 22:8664–74. doi: 10.26355/eurrev_201812_16631
 67. Rastgoo N, Pourabdollah M, Abdi J, Reece D, Chang H. Dysregulation of EZH2/miR-138 axis contributes to drug resistance in multiple myeloma by downregulating RBPM5. *Leukemia.* (2018) 32:2471–82. doi: 10.1038/s41375-018-0140-y
 68. Tang X, Jiang J, Zhu J, He N, Tan J. HOXA4-regulated miR-138 suppresses proliferation and gefitinib resistance in non-small cell lung cancer. *Mol Genet Genomics.* (2018) 294:85–93. doi: 10.1007/s00438-018-1489-3
 69. Jiang B, Xu G, Lv HQ, Huang M, Li Z. Up-regulation of miR-765 predicts a poor prognosis in patients with esophageal squamous cell carcinoma. *Eur Rev Med Pharmacol Sci.* (2018) 22:3789–94. doi: 10.26355/eurrev_201806_15261
 70. Lin J, Zhang D, Fan Y, Chao Y, Chang J, Li N, et al. Regulation of cancer stem cell self-renewal by HOXB9 antagonizes endoplasmic reticulum stress-induced melanoma cell apoptosis via the miR-765-FOXA2 axis. *J Invest Dermatol.* (2018) 138:1609–19. doi: 10.1016/j.jid.2018.01.023
 71. Liang W, Wei X, Li Q, Dai N, Li CY, Deng Y, et al. MicroRNA-765 enhances the anti-angiogenic effect of CDDP via APE1 in osteosarcoma. *J Cancer.* (2017) 2:1542–51. doi: 10.7150/jca.18680
 72. Zheng Z, Luan X, Zha J, Li Z, Wu L, Yan Y, et al. TNF- α inhibits the migration of oral squamous cancer cells mediated by miR-765-EMP3-p66Shc axis. *Cell Signal.* (2017) 34:102–9. doi: 10.1016/j.cellsig.2017.03.009
 73. Xie BH, He X, Hua RX, Zhang B, Tan GS, Xiong SQ, et al. Mir-765 promotes cell proliferation by downregulating INPP4B expression in human hepatocellular carcinoma. *Cancer Biomark.* (2016) 16:405–513. doi: 10.3233/CBM-160579

Conflict of Interest Statement: The authors declare that the research was conducted in the absence of any commercial or financial relationships that could be construed as a potential conflict of interest.

Copyright © 2019 Salinas-Vera, Gallardo-Rincón, García-Vázquez, Hernández-de la Cruz, Marchat, González-Barrios, Ruíz-García, Vázquez-Calzada, Contreras-Sanzón, Resendiz-Hernández, Astudillo-de la Vega, Cruz-Colin, Campos-Parra and López-Camarillo. This is an open-access article distributed under the terms of the Creative Commons Attribution License (CC BY). The use, distribution or reproduction in other forums is permitted, provided the original author(s) and the copyright owner(s) are credited and that the original publication in this journal is cited, in accordance with accepted academic practice. No use, distribution or reproduction is permitted which does not comply with these terms.